MSDE

PAPER

View Article Online
View Journal

Cite this: DOI: 10.1039/d5me00074b

Bioinspired nucleolipid as a low molecular weight oleogelator for oil-in-water nanoemulsions

Arthur Klufts-Edel,†[a] Bérangère Dessane,†[a] Ahmad Saad,[b] Nadia El Mammeri,[b] Antoine Loquet,[b] Brice Kauffmann,[c] Muriel Cario,[de] Philippe Barthélémy,[a] Fanny Caffin,[f] Christophe Piérard,[f] Sylvie Crauste-Manciet *[ag] and Valérie Desvergnes *[a]

Received 28th April 2025,
Accepted 1st January 2026

DOI: 10.1039/d5me00074b

rsc.li/molecular-engineering

Low molecular-weight organogels are particularly attractive soft materials for drug delivery, tissue engineering, environmental remediation and the food industry. In this study, we describe a molecular approach to develop nucleolipid (NL) as a novel low molecular weight oleogelator (LMWO). NL **5** demonstrated self-assembling properties, forming a three-dimensional solid-like network that traps a substantial amount of the carrier oil solvent and enables the creation of an oleogel. As a bio-inspired, low molecular-weight oleogelator, NL **5** was able to stabilize thixotropic medium chain triglyceride (MCT)-based oleogels at low concentrations (1.5% w/w). Furthermore, this NL also induced the gelation of an oil-in-water nanoemulsion, resulting in a novel oleogel-based nanoemulsion through supramolecular interactions. Unlike common strategies that rely on trapping the dispersed phase by gelation of the continuous phase, we report an innovative oil-in-water nanoemulsion obtained *via* gelation of dispersed oil droplets. These oil droplets form an oleogel through LMWO based on NL, which is used at a remarkably low final concentration (1% w/w). The bio-inspired and biocompatible nature of this oleogelator, along with its efficiency at low concentrations and its ability to gel a nanoemulsion, makes it particularly appealing for further cosmetic and pharmaceutical developments.

Design, System, Application

This work focuses on designing a novel bio-inspired low molecular weight oleogelator (LMWO) based on nucleolipids (NLs). Using a molecular approach, NL 5 was developed to self-assemble and create a three-dimensional solid-like network within oil, forming the first reported NL-based oleogel. The synthesis of NL 5 was carried out through an efficient, streamlined 5-step sequence, producing a versatile oleogelator with remarkable self-assembling properties. Its bio-inspired design ensures biocompatibility, making it a promising material for applications in fields requiring sustainable and adaptable soft materials. The system involves NL 5 functioning as a supramolecular oleogelator to stabilize thixotropic medium chain triglyceride (MCT)-based oleogels at low concentrations (1.5% w/w). Furthermore, NL 5 induced the gelation of oil-in-water nanoemulsions by forming oleogel droplets through supramolecular interactions. Unlike conventional systems where gelation occurs in the aqueous continuous phase, this method innovatively targets dispersed oil droplets to achieve stabilization, with a remarkably low concentration of NL 5 (1% w/w) in the oil phase. The dual ability of NL 5 to stabilize oleogels and nanoemulsions highlights its versatility within multiphasic systems. This innovative oleogelator holds significant potential for applications across diverse fields. Its ability to stabilize thixotropic oleogels and induce nanoemulsion gelation presents opportunities for drug delivery systems, offering efficient encapsulation and release properties. In the cosmetics industry, NL 5's biocompatibility and performance at low concentrations make it suitable for formulations requiring soft, adaptive materials. Ther industries could also benefit from its bio-inspired nature and scalable synthesis. This work sets the stage for further exploration of NL-based materials as advanced soft matter platforms for cosmetic, pharmaceutical, and industrial applications.

Introduction

Supramolecular gels derived from low molecular weight gelators (LMWGs), formed through physical and reversible crosslinking, have garnered increasing attention as an alternative to polymer-based gels,[1–9] due to improved biocompatibility and greater synthetic tuneability. Recent literature in this field reports the existence of flexible biomolecule-derived[10–12] materials, including peptides,[13–20] carbohydrates,[21–25] and nucleic acid derivatives.[26–28] The supramolecular properties of these biomolecules make them

[a] CNRS, INSERM, ARNA, UMR 5320, Univ. Bordeaux, U1212, F-33000 Bordeaux, France. E-mail: sylvie.crauste-manciet@univ-angers.fr, valerie.desvergnes@u-bordeaux.fr
[b] CNRS, Bordeaux INP, CBMN, Univ. Bordeaux, UMR 5248, F-33600 Pessac, France
[c] CNRS, INSERM, IECB, Univ. Bordeaux, US1, UAR 3033, F-33600 Pessac, France
[d] INSERM, BRIC, Univ. Bordeaux, U 1312, F-33000 Bordeaux, France
[e] AquiDerm, University of Bordeaux, Bordeaux, France
[f] Institut de Recherche Biomédicale des Armées, 1 place du Général Valérie André, 91220 Brétigny-sur-Orge, France
[g] INSERM, CNRS, MINT, SFR ICAT, University of Angers, [CHU Angers], F-49000 Angers, France
† These authors contributed equally to this work.

highly interesting for various applications,[29–31] especially in materials[32,33] and medical science.[34] Among synthetic bioconjugates, nucleolipids (NL),[35–37] consisting of nucleic acids with a covalently linked lipid moiety to a nucleoside or nucleotide, are hybrid molecules inspired by natural structures existing in biological systems. Nucleolipids represent promising supramolecular tools as they can engage in numerous weak interactions.[38–42] These bioinspired amphiphilic hybrids combine the aggregation behavior of lipids with the specific recognition functions of nucleosides, making them uniquely suited to organize into supramolecular structures This natural occurrence, their remarkable self-assembly properties served as the conceptual foundation for our bioinspired design of gelator molecules. This strategy not only enables functionalization to finely tune gelation properties but also increases the likelihood of biocompatibility.

While numerous examples of LMWGs have been formed primarily in water and organic solvents,[7,31,43–46] a supramolecular approach could prove highly interesting for stabilizing oleogels. Oleogels are organogels in which an oil phase is trapped within a network of organic gelator molecules. They have emerged as promising biocompatible drug delivery systems (DDS) for the administration of hydrophobic active pharmaceutical ingredients (APIs). In contrast to organogels that utilize organic solvents, oleogels employing edible oils are biocompatible, eliminating the need for removal of toxic organic compounds.[47] They offer versatile routes of administration, including transdermal, oral, and parenteral, making them suitable for sustained drug delivery.[48] Compared to hydrogels, which often exhibit rapid drug release from the hydrophilic matrix, oleogels facilitate sustainable drug release from the oil phase. Oleogels are attracting growing interest as DDS because they also offer distinct and complementary advantages over hydrogels, such as higher mechanical strength and greater loading capacity for lipophilic drugs.[48] The potential of low molecular weight oleogels (LMWO) has been highlighted through several promising examples of self-assembled soft matter,[49–51] particularly as alternatives to organogels derived from organic solvents. The ability of a low molecular weight gelator to act as an oleogelator is linked to its solubility in the oil phase. Some oleogelators bioderived from carbohydrates, fatty acids, or amino acids have been described.[52,53] The development of novel synthetic families of oleogelators, readily modified, would offer exciting opportunities to tune the physicochemical properties of LMWO. To our knowledge, there are no previous examples of nucleic acid-based oleogelators.

Our team possesses extensive expertise in the synthesis of amphiphilic NL hydrogelators and organogelators.[54–56] In this communication, we first present the design and synthesis of oil–soluble lipophilic NLs and their physicochemical properties as LMWOs (low molecular weight organogelators). Among lipid-based formulations, nanoemulsions (NEs) have gained increasing interest over the past decade for the delivery of lipophilic drugs.[57] NEs are fine dispersions of small droplets (between 100 and 500 nm) of two immiscible liquids, oil in water (O/W) or water in oil (W/O), stabilized by a surfactant.

O/W or W/O NEs ability to simultaneously incorporate hydrophilic and lipophilic active ingredients makes them highly versatile, although their inherent thermodynamic instability remains a major limitation.[58] Amongst stabilization methods, external phase gelation has been developed to produce nanoemulgel with improved pharmacokinetic outcomes for lipid-based drugs.[59] The development of nanoemulsions based on oleogels, which combine the benefits of oleogels and nanosystems, presents a remarkable challenge. By enabling substantial viscosity tuning of the gels and simultaneous, facile loading of hydrophilic and hydrophobic compounds with well-defined phases, oleogels broaden the application scope comparable to liquid nanoemulsions.

To date, various gel-based systems have been reported for topical or oral administration of bioactive compounds. Some are emulsion-based gels, employing a gelator in the aqueous continuous phase to produce nanoemulgels[60] while others formed bigels combining gelified nanoemulsions with oleogels.[61] However, our approach described herein stands apart from these systems through the development of an efficient nucleolipd-based LWMG stabilizing the oleogel of the oil-in-water nanoemulsion.

In this work, we present a distinct approach in which a synthetic nucleolipid-based LMWO is incorporated into the internal oil phase of an O/W nanoemulsion, forming a stabilized oleogel. This strategy provides an efficient means of overcoming instability issues while broadening the potential of lipid-based nanosystems for biomedical applications.

Results and discussion

Given the multiplicity of factors that can influence the formation of a non-covalent self-assembled fibrillar network (SAFiN) from LMWO in solution, designing a structure that achieves the optimal balance of weak physical interactions remains a major challenge.[62] Most examples of gelators reported in the literature have been discovered thanks to serendipity.[63] Thus, it is essential to gain a deeper understanding of how the chemical structure of the gelator affects the self-assembly of typically fibrous structures and the subsequent gelation of a solvent.

This work underscores how a minute structural change, such as the nature of an atom, finely modulates molecular behaviour and radically alters the properties of a supramolecular assembly.

Previous unpublished work of our team highlighted the ability of NLs bearing 1,4 dicarbonyl spacers to self-assemble when dispersed in oils. To better understand the structural factors governing the gelation process, we have synthesized three NL-based compounds. Using a straightforward synthetic approach, we performed the synthesis (Fig. 1) of

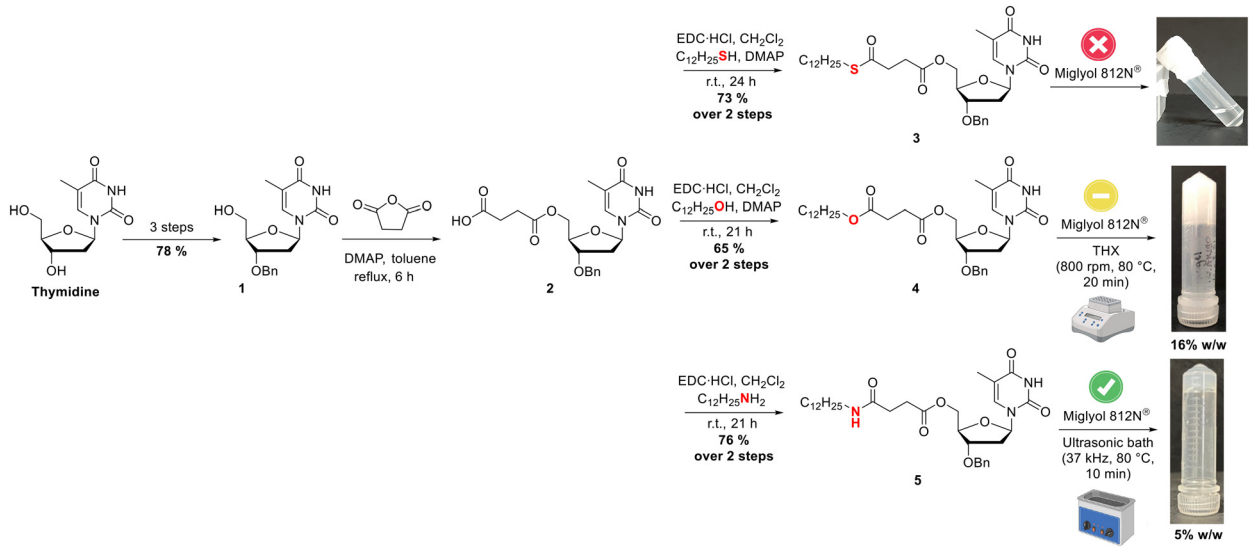

Fig. 1 Synthetic sequence providing NL **3**, NL **4** and NL **5** and subsequent oleogel formulation.

the thymidine-based NL 3–5 featuring a 1,4-dicarbonyl linkage. All the compounds were obtained *via* the same five-step efficient sequence. The intermediate benzylated ether **1** was submitted to classical anhydride desymmetrization conditions[64] providing the succinate derivative **2**. The last step to install the fatty chain used a Steglich-like coupling reaction from the convenient 1-dodecanethiol, 1-dodecanol and dodecylamine leading respectively to compound **3** bearing an ester-thioester linkage, compound **4** bearing a diester and **5** bearing an ester-amide link. Gelation properties investigation highlighted that **3** was not soluble in the MCT oil solvent (Miglyol® 812 N). Using the same gelation protocol, compound **4** was found to provide an unstable gel over time at the relatively high concentration of 16% w/w. Within 30 days, oleogel syneresis was visually observed.

Finally, compound **5** led to the formation of a stable oleogel from pharmaceutical Miglyol® 812 N at a remarkable concentration of 1.5% w/w. Indeed, a translucid-like gel was obtained after only 5 minutes when compound **5** was used at 5% w/w final concentration. The macroscopic observation showed a white, opaque gel for NL **4** and a translucent gel for NL **5** as early as 1.5% w/w. Optical microscopy revealed twisted micron-sized fibers network (Fig. 2).

In order to get insight into the structural features of the self-assembly, we carried out solution and solid-state NMR experiments under magic-angle spinning conditions and compared ^{13}C-detected solid-state NMR experiments of the oleogels resulting from **4** and **5** to solution NMR experiment on the Miglyol® 812 N oil (Fig. 3). We performed two types of polarization transfer for the oleogel: a ^{1}H–^{13}C cross-polarization (CP) revealing rigid moieties and a ^{1}H–^{13}C INEPT to detect mobile moieties. Noticeably, the nucleobase and the fatty chain unambiguously constitute the rigid part of the oleogel as they are only detected in the CP experiment. The Miglyol® 812 N oil undergoes a highly mobile regime in the gel, as observed in the INEPT experiment. NMR resonances were fully assigned for NL **5** even if the CP spectra exhibited lower resolution compared to those of NL **4**. In the case of NL **4** the observation of sharp ^{13}C lines suggest the presence of a single rigid conformation within the oleogel assembly.

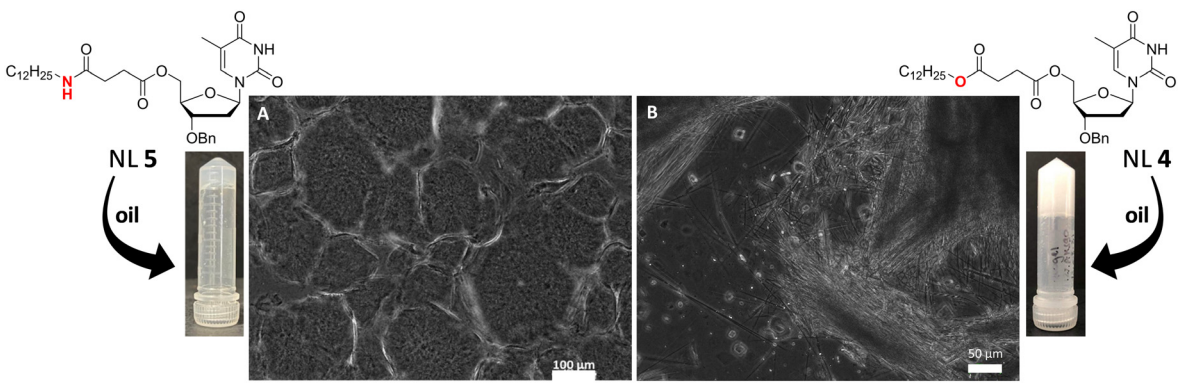

Fig. 2 Microscopic optical observations of NL **5** (5% (w/w) (A) and NL **4** (16% (w/w) (B) -based oleogels in MCT oil (Miglyol® 812 N) showing crystalline fiber's network.

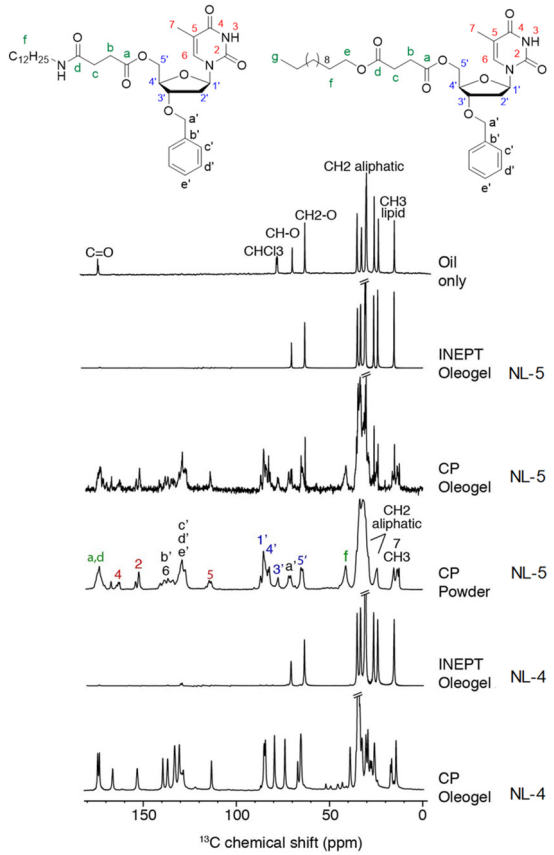

Fig. 3 From top to bottom: ^{13}C NMR spectra of the Miglyol oil, INEPT and CP ^{13}C NMR spectra of the oleogel resulting from **5**. CP ^{13}C NMR spectra of **5** at the solid state. INEPT and CP ^{13}C NMR spectra of the oleogel resulting from **4**.

Crystals extracted from the compound **3** insoluble in oil and from **4** based oleogel were investigated and confirmed a supramolecular assembly resulting from two very similar quasi-perfect packings of nucleobases and fatty chains. In both crystal structures the packing is stabilized by the same network of hydrogen bonds involving water molecules and the nucleobases moiety (Fig. 4 and SI Fig. S10 and S11).

Only the positions of the fatty acids' chains are slightly different explaining the space group transition from orthorhombic P212121 (compound **3**) to monoclinic P21 (compound **4**) (see SI Fig. S12). These observations are in line with the solid-state CP-NMR data of gels resulting from **4** and **5**, also demonstrating the very rigid and well-ordered arrangement of these moieties in the crystal. Even although we cannot explain it, the resolution of the NMR spectrum is lower for gel **5**. Understanding the crucial role of the NH moiety in the present case could provide insights to rationalize the design of such LMWO materials.[65] Surprisingly, obtaining a single crystal structure from the oleogel derived from **5** proved elusive. However, the wide-angle X-ray diffraction pattern (see SI Fig. S9) measured on NL **5** based oleogel is in accordance with a bidimensional lamellar-like structure as shown by the best indexation calculation giving a monoclinic crystal lattice with an *a*-axis of 36 Å compatible with the interlamellar spacing periodicity. The lower resolution of the NMR spectrum for **5** derived oleogel could be related to the poor periodicity in the smectic planes as confirmed by the X-ray data. With no further structural evidence supporting NH involvement in H-bonding and considering the extensive literature on various organogels and hydrogels containing an amide,[66–71] we can only hypothesize that such a functional group might play a decisive role during the nucleation process. Despite the partial and unsatisfactory gelation of NL **4**, we can assume that the molecular arrangement is primarily governed by hydrophobic interactions between the monomers of NL **4**.

Rheological studies provided information regarding the overall stiffness and the mechanical strength properties of the NL **5** based oleogel at 5% (w/w) in Miglyol® 812 N (Fig. 5). G′ values are higher than G″ (Fig. 5A) throughout the frequency range considered, without crossing each other, indicating a solid-like character of the oleogel at 5% (w/w) in

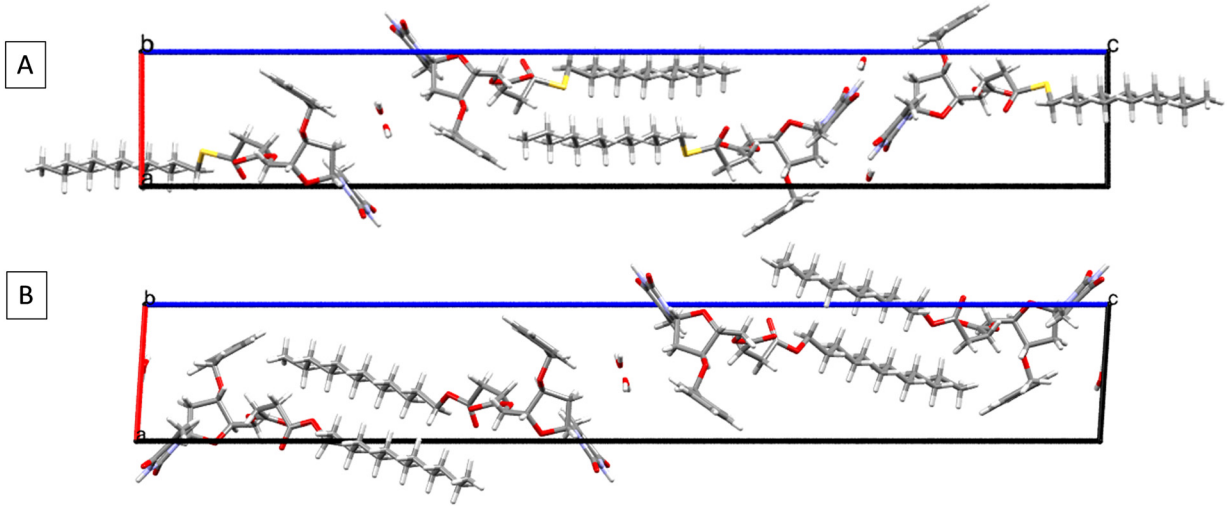

Fig. 4 View along the *b* axis of the crystal structure of A) compound **3** in suspension in MCT oil and B) partially gelled compound **4** in MCT oil.

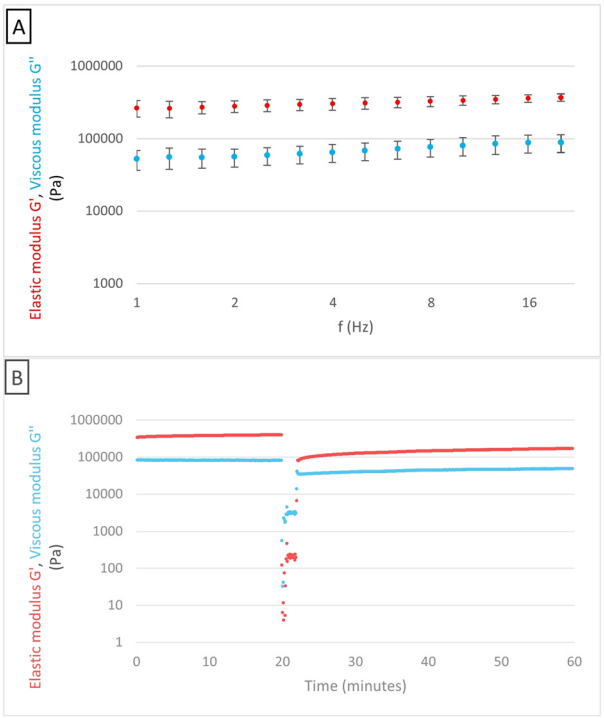

Fig. 5 A-frequency sweep experiment of NL **5** based oleogel 5% w/w in Miglyol® 812 N. B- step-strain experiment of NL **5** based oleogel 5% w/w in Miglyol® 812 N at a fixed shear strain of 0.1%.

Miglyol® 812 N ($G' = 2.82 \times 10^5$ Pa, $G'' = 5.61 \times 10^4$ Pa). The quite high G′ and G″ values were also weakly dependent on the frequency across the entire range. The studies into the possible thixotropic behavior of this oleogel demonstrated that the material exhibiting a fluid-like behavior while under stress was able to revert to a gel state when at rest (Fig. 5B). This property is particularly interesting for therapeutic applications requiring injectable gels with tunable rheological properties. The Tgel–sol transition temperature was of 79.5 °C (Fig. 6), in accordance with the dissolution temperature used to form the gel. The CGC characterization highlighted a very interesting property of NL **5** in Miglyol® 812 N. Indeed, a variation of the concentration generated modification in gelation time between 1.5 h at 1.5% w/w to 5 minutes at 5% w/w. Tunability of gelation time is of great interest for pharmaceutical manufacturing (See SI for complementary rheological results of NL **5** at 5% Fig. S3 and 2%, Fig. S4–S6). In fact, for gelled NE, we chose the 5% w/w concentration in the oil to allow the fastest gelation time to minimize phase change during the process.

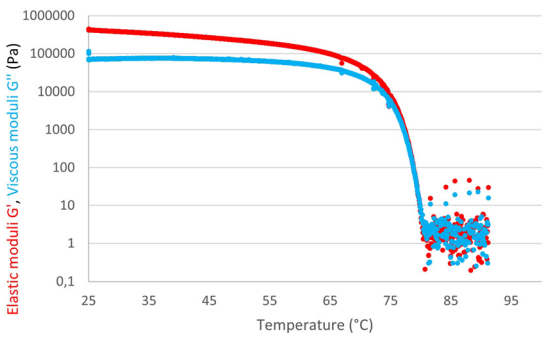

Fig. 6 Tgel/sol transition temperature of 5% w/w NL 5-based oleogel.

In an effort to explore a method different from existing ones for developing gelled nanoemulsions, the original biocompatible (see cytotoxicity results SI Fig. S12) synthetic gelator nucleolipid-based NL **5** was then incorporated into the oil phase of the oil-in-water nanoemulsion. This specific strategy resulted in the formation of a stabilized oleogel within the nanoemulsion (Fig. 7C and SI Fig. S7 for picture of gelled NE-NL **5**).

The particle size characteristics were good and comparable between the two formulas with and without NL, although the mean diameter values were slightly reduced, suggesting stabilization by NL (see SI Table S1 for composition and Table S2 for characteristics). Nanoemulgels have been employed to facilitate and promote topical[60] as well as oral administration. Formulations based on oleogels represent an alternative system wherein gelation occurs in the oil phase.[72]

In our study, we formulated a gelled O/W nanoemulsion using an original synthetic oleogelator located in the oil phase, differentiating our system from previously described ones, and providing additional value. Our developed system stands apart from nanoemulgels where the aqueous phase is gelled by a hydrogelator, resulting in the dispersion of liquid oil droplets in a water gel matrix. The literature has also described what is called a bigel, where both phases are gelled: both the oil droplets and the continuous aqueous phase are gelled using hydrogelators and oleo- or organogelators, respectively.[73] Remarkably, in our study, both phases were gelled using a single gelator. The gelation of the aqueous phase was notably confirmed by microscopic observation of the NE, wherein a dense network of fibers was observed (Fig. 7).

The exceptional aspect lies in the fact that our synthetic oleogelator is insoluble in water. A specific gelation mechanism was initially proposed for another low-molecular-weight gelator, 12-hydroxyoctadecanoic acid (12 HOA).[74] The authors observed that when bioderived 12 HOA was dispersed in Miglyol® 812 within a nanoemulsion, it first underwent self-assembly within the oil droplets. Due to the high concentration and close proximity of the oil droplets, the gel network was able to propagate into the aqueous phase. A similar gelation

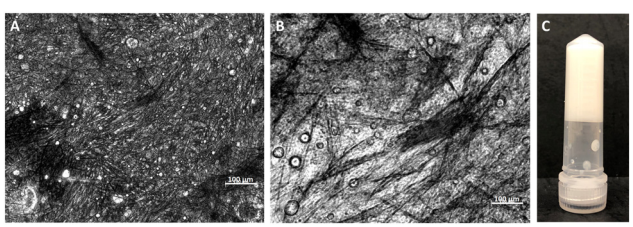

Fig. 7 Microscopic optical observation of gelled NE-NL **5** based at ×10 (A) and ×20 (B) magnification and macroscopical aspect of gelled NE-NL **5** (C).

phenomenon has been reported for the low molecular weight organogelator 12-hydroxystearic acid (12-HSA),[75] where gelation occurs in both phases of a macroemulsion. This process was attributed to the migration of 12-HSA molecules from the oil phase to the water phase through interfacial electrostatic interactions, subsequently leading to the formation of self-assembled structures and fiber networks in the aqueous phase. In the case of 12 HOA nanoemulsion, the self-assembly observed in the aqueous phase occurred slowly, resulting in the initial formation of a weak gel, which eventually developed into a stable gel after 3 days.

Remarkably, our formulation demonstrated a much more rapid gelation, achieving a perfectly stable gel in just 2 hours. Furthermore, while both formulations have a final NL **5** oleogelator concentration of 1% in the nanoemulsion, a closer examination of the oleogelator-to-oil phase ratio revealed a striking difference. The formulation based on 12 HOA contains a 20% oleogelator ratio, whereas a mere 5% of our synthetic compound in the oil phase is sufficient to achieve efficient gelation in the described case.

With 5% oleogelator concentration in the oil, resulting in 1% final concentration in the NE, we observed a 10^2 reduction in the stiffness of the moduli G′ and G″ of our corresponding oleogel (G′ = $3.7.10^3$ Pa, G″ = 716 Pa) (Fig. 8 and SI Fig. S8). However, compared to the 12 HOA NE formulation, our stiffness expressed by G′ was a power of ten higher. The macroscopic aspect of the gelled NE was noticeably stable over 4 months at room temperature.

The presence of lecithins in the formulation could potentially function as a co-oleogelator, as previously reported,[76] and might contribute to the observed gelation rate and stiffness in our gelled nanoemulsion formulation. Nevertheless, comprehensive investigations are warranted to completely elucidate the mechanistic intricacies underlying the gelation induced by our novel synthetic NL-based oleogelator.

Experimental

Synthetic procedures: synthesis and characterization of compounds 1–5

General methods. ^{1}H NMR and ^{13}C NMR were recorded on a Bruker Avance 300 (^{1}H: 300 MHz, ^{13}C: 75.46 MHz) spectrometer using residual CHCl3 as an internal reference (7.26 ppm) and at 293 K unless otherwise indicated. The chemical shifts (δ) and coupling constants (J) are expressed in ppm and Hz. The following abbreviations were used to explain the multiplicities: *s* = singlet, *d* = doublet, *t* = triplet, *q* = quartet and *m* = multiplet. Fourier transform infrared (FT-IR) spectra were recorded on a PerkinElmer FT spectrometer spectrum two (UATR two). For electrospray ionization (ESI) high-resolution mass spectrometry (HRMS) analyses, a waters micromass ZQ instrument equipped with an electrospray source was used in the positive and/or negative mode. Matrix-assisted laser desorption ionization time-of-flight (MALDI-TOF) mass spectrometric analyses were performed on a PerSeptive Biosystems Voyager-De Pro MALDI mass spectrometer in the linear mode using 3,4-dihydroxybenzoic acid as the matrix. Analytical thin-layer chromatography was performed using silica gel 60 F254 precoated plates (Merck) with visualization by ultraviolet light, potassium permanganate, or sulfuric acid. Flash chromatography was performed on a silica gel (0.043–0.063 mm).

Synthesis of compound 1. Three step-sequence synthesis of 3-benzylated alcohol **1**.

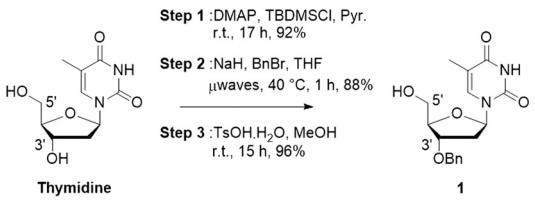

Step 1: To a solution of thymidine (10 g, 41.28 mmol, 1.0 eq.) in pyridine (0.05 g mL^{-1}, 200 mL) was added DMAP (catalytic amount) and *tert*-butyldimethylsilyl chloride (7.47 g, 49.54 mmol, 1.2 eq.) sequentially. The reaction mixture was stirred during 17 h at room temperature. After removal of the solvent under reduced pressure, the crude reaction mixture was dissolved in DCM and washed successively with water, saturated solution of $NaHCO_3$ and brine. The organic layer was dried over Na_2SO_4 and evaporated under reduced pressure. The crude product was recrystallized in CH_2Cl_2/pentane to afford pure silyl ether as a white solid (13.49 g, 37.84 mmol, 92%). Data were consistent with literature.

Step 2: In a vial, NaH (60% dispersion in oil, 280 mg, 7.01 mmol, 2.5 eq.) was added by portions at 0 °C to a solution of the previously obtained silylated compound (1 g, 2.80 mmol, 1.0 eq.), in THF (0.1 g mL^{-1}, 10 mL) and the reaction mixture was activated under microwaves (CEM machine, 200 watts) at 40 °C during 4.5 minutes. Benzyl bromide (833 μL, 7.01 mmol, 2.5 eq.) was then added and the reaction medium was submitted to a second microwave activation time (60 minutes, 40 °C, 200 watts). After being cooled at room temperature, the reaction was quenched with a saturated aqueous solution of NH_4Cl and DCM was added. The

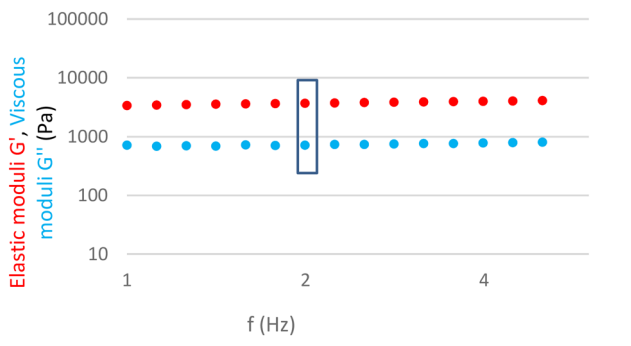

Fig. 8 Frequency sweep experiment of gelled NE with NL **5** at 5% w/w in Miglyol® 812 N.

aqueous layer was extracted three times with DCM 3 times. The combined organic extracts were then dried over Na_2SO_4 and filtered. Concentration under reduced pressure afforded the crude product which was then purified by flash chromatography over silica gel (pentane/EtOAc 70/30) to afford the desired product as a colorless gum (1.013 g, 2.27 mmol, 88%). Data were consistent with literature.

Step 3: Compound from step 2 was dissolved in MeOH (0.1 g mL^{-1}, 9 mL) and para-toluenesulfonic acid (monohydrated, 86 mg, 0.45 mmol, 0.2 eq.) was added. The reaction mixture was then stirred at room temperature during 15 h before being concentrated under reduced pressure, dissolved in CH_2Cl_2, washed with a saturated aqueous solution of $NaHCO_3$ and brine. The combined organic extracts were dried over Na_2SO_4 and filtered. Concentration under reduced pressure afforded the crude product which was then purified by flash chromatography over silica gel (CH_2Cl_2/MeOH 95/5) to give 3′-benzylated thymidine compound **1** as a white solid (724 mg, 2.18 mmol, 96%).

Mp: 141 °C; Rf = 0.25 (pentane/EtOAc 30/70); IR (ATR) ν_{max} (cm^{-1}) 3422, 3186, 3062, 3038, 2928, 1683,1471, 1405, 1366, 1324, 1275, 1203, 1132, 1096, 1058, 960, 910, 787, 736, 699, 651, 606, 560, 492; ^{1}H-NMR (300 MHz, $CDCl_3$) δ (ppm) 8.99 (s, 1H, NH-3), 7.42–7.29 (m, 6H, H_6/$H_{aromatic}$), 6.14 (dd, J = 6.6, 7.5 Hz, 1H, $H_{1'}$), 4.54 (AB system, J = 11.8 Hz, 2H, $H_{a'}$), 4.33–4.26 (m, 1H, $H_{4'}$), 4.20–4.13 (m, 1H, $H_{3'}$), 3.93 (dd, J = 2.4, 11.7 Hz, 1H, $H_{5'a}$), 3.75 (dd, J = 3.0, 12 Hz, 1H, $H_{5'b}$), 2.48–2.28 (m, 2H, $H_{2'}$), 1.90 (s, 3H, H_7); ^{13}C-NMR (75.5 MHz, $CDCl_3$) δ (ppm) 163.9 (C_4), 150.5 (C_2), 137.6 (C_6), 137.2 ($C_{b'}$), 128.7 ($C_{d'}$), 128.1 ($C_{e'}$), 127.8 ($C_{c'}$), 111.2 (C_5), 87.5 ($C_{1'}$), 85.3 ($C_{4'}$), 78.7 ($C_{3'}$), 71.8 ($C_{a'}$), 62.9 ($C_{5'}$), 37.3 ($C_{2'}$), 12.6 (C_7); HRMS (ESI): Calcd. for $C_{17}H_{20}N_2O_5Na$ $[M + Na]^+$ 355.12644, found 355.12650.

Synthesis of compound 2. DMAP (cat. amount) and succinic anhydride (301.1 mg, 3.01 mmol, 1 eq.) were successively added to a stirred suspension of **1** (1.00 g, 3.01 mmol, 1 eq.) in toluene (0.044 M, 68.4 mL). The mixture was stirred at reflux during 6 h. The reaction mixture was allowed to cool down to room temperature before being concentrated under reduced pressure. Crude **2** was isolated as a white foam (1.52 g) and submitted to the next step without further purification.

Synthesis of compound 3. Dodecanethiol (994 µL, 4.15 mmol, 3.5 eq.), DMAP (58 mg, 0.47 mmol, 0.4 eq.) and EDC.HCl (568 mg, 2.96 mmol, 2.5 eq.) were successively added to a stirred solution of acid 2 (513 mg, 1.19 mmol, 1 eq.) in CH_2Cl_2 (0.1 M, 11.9 mL). The mixture was stirred at room temperature during 24 h. The reaction mixture was quenched with a saturated solution of NH_4Cl and CH_2Cl_2 was added. The aqueous layer was extracted 3 times with CH_2Cl_2. Combined organic layers were dried over Na_2SO_4 and filtered. Concentration under reduced pressure afforded the crude product. The crude product was purified by flash chromatography over silica gel (EtOAc/pentane 40/60 to 50/50) to afford thioester **3** as a yellow gum (405 mg, 0.66 mmol, 73% over 2 steps from 1).

Rf = 0.36 (EtOAc/P 4/6); IR (ATR) ν_{max} (cm^{-1}) 3182, 2923, 2860, 1684, 1460, 1372, 1268, 1194, 971, 897, 738, 608, 480, 414; ^{1}H-NMR (300 MHz, $CDCl_3$) δ (ppm) 9.67 (s, 1H, NH-3), 7.41–7.19 (m, 6H, H_6/$H_{aromatics}$), 6.27 (dd, J = 6.0, 7.5 Hz, 1H, $H_{1'}$), 4.53 (AB system, J = 11.7 Hz, 2H, $H_{a'}$), 4.36 (dd, J = 5.4, 12.9 Hz, 1H, $H_{5'a}$), 4.30–4.21 (m, 2H, $H_{4'}$/$H_{5'b}$), 4.16–4.07 (m, 1H, $H_{3'}$), 2.94–2.81 (m, 4H, H_c/H_d), 2.67–2.62 (m, 2H, H_e), 2.50 (ddd, J = 3.0, 6.0, 13.8 Hz, 1H, $H_{2'a}$), 2.12–1.99 (m, 1H, $H_{2'b}$), 1.92 (d, J = 1.2 Hz, 3H, H_7), 1.60–1.47 (m, 2H, H_f), 1.38–1.15 (m, 18H, $H_{aliphatics}$), 0.92–0.78 (m, 3H, H_g); ^{13}C-NMR (75.5 MHz, $CDCl_3$) δ (ppm) 197.9 (C_d), 171.7 (C_a), 164.0 (C_4), 150.4 (C_2), 137.3 ($C_{b'}$), 135.2 (C_6), 128.6 ($C_{d'}$), 128.1 ($C_{e'}$), 127.8 ($C_{c'}$), 111.3 (C_5), 85.4 ($C_{1'}$), 82.2 ($C_{4'}$), 78.4 ($C_{3'}$), 71.8 ($C_{a'}$), 64.2 ($C_{5'}$), 38.3 (C_c), 37.6 ($C_{2'}$), 32.0 ($C_{aliphatic}$), 29.7 (C_b), 29.6 ($C_{aliphatic}$), 29.5 ($C_{aliphatic}$), 29.4 ($C_{aliphatic}$), 29.2 ($C_{aliphatic}$), 29.1 ($C_{aliphatic}$), 28.9 (C_f), 22.7 ($C_{aliphatic}$), 14.2 (C_g), 12.7 (C_7); HRMS (ESI): Calcd for $C_{33}H_{48}N_2O_7S$ $[M + H]^+$, 617.32635, found 617.48023.

Synthesis of compound 4. Acid **2** (1.51 g, 3.50 mmol, 1.5 eq.), DMAP (171.5 mg, 1.40 mmol, 0.6 eq.) and EDC.HCl (671.0 mg, 3.50 mmol, 1.5 eq.) were successively added to a stirred solution of dodecanol (430.2 mg, 2.33 mmol, 1 eq.) in DCM (0.1 g mL^{-1}, 4.5 mL). The mixture was stirred at room temperature during 21 h. The reaction mixture was quenched with a saturated solution of NH_4Cl and CH_2Cl_2 was added. The aqueous layer was extracted 3 times with CH_2Cl_2. Combined organic layers were dried over Na_2SO_4 and filtered. Concentration under reduced pressure afforded the crude product. The crude product was purified by flash chromatography over silica gel (EtOAc/pentane 50/50) to afford ester **4** as a white solid (913.4 mg, 1.52 mmol, 65% over 2 steps from 1).

Mp: 64–66 °C; Rf = 0.32 (EtOAc/P 40/60); IR (ATR) ν_{max} (cm^{-1}) 3171, 3042, 2921, 2857, 1693, 1460, 1367, 1216, 1151, 1081, 969, 869, 739, 650, 598, 557, 488; ^{1}H-NMR (300 MHz, $CDCl_3$) δ (ppm) 9.25 (s, 1H, NH-3), 7.40–7.27 (m, 6H, H_6/$H_{aromatics}$), 6.28 (dd, J = 6.0, 7.5 Hz, 1H, $H_{1'}$), 4.53 (AB system, J = 11.7 Hz, 2H, $H_{a'}$), 4.43–4.34 (m, 1H, H_{e1}), 4.31–4.22 (m, 2H, H_{e2}/$H_{4'}$), 4.16–4.10 (m, 1H, $H_{3'}$), 4.06 (t, J = 6.6 Hz, 2H, $H_{5'}$), 2.71–2.56 (m, 4H, H_b/H_c), 2.51 (ddd, J = 3.0, 6.0, 13.8 Hz, 1H, $H_{2'a}$), 2.12–2.01 (m, 1H, $H_{2'b}$), 1.92 (d, J = 1.2 Hz, 3H, H_7),1.67–1.54 (m, 2H, H_f), 1.38–1.17 (m, 18H, $H_{aliphatic}$), 0.95–0.80 (m, 3H, H_g); ^{13}C-NMR (75.5 MHz, $CDCl_3$) δ (ppm) 172.3 (C_d), 172.1 (C_a), 163.9 (C_4), 150.4 (C_2), 137.3 ($C_{b'}$), 135.3 (C_6), 128.7 ($C_{d'}$), 128.2 ($C_{e'}$), 127.8 ($C_{c'}$), 111.3 (C_5), 85.4 ($C_{1'}$), 82.3 ($C_{4'}$), 78.4 ($C_{3'}$), 71.8 ($C_{a'}$), 65.2 ($C_{5'}$), 64.2 (C_e), 37.7 ($C_{2'}$), 32.0 ($C_{aliphatic}$), 29.7 ($C_{aliphatic}$), 29.7 ($C_{aliphatic}$), 29.7 ($C_{aliphatic}$), 29.6 ($C_{aliphatic}$), 29.4 ($C_{aliphatic}$), 29.3 ($C_{aliphatic}$), 29.1 (C_c), 29.0 (C_b), 28.7 (C_f), 26.0 ($C_{aliphatic}$), 22.8 ($C_{aliphatic}$), 14.2 (C_g), 12.7 (C_7); HRMS (ESI): Calcd. for $C_{33}H_{48}N_2O_8$ $[M + NH_4]^+$, 618.37489, found 618.37420.

Synthesis of compound 5. Dodecyl amine (595 µL, 2.59 mmol, 1.4 eq.) and EDC.HCl (496.1 mg, 2.59 mmol, 1.4 eq.) were successively added to a stirred solution of acid **2** (799.4 mg, 1.85 mmol, 1 eq.) in CH_2Cl_2 (0.17 M, 10.87 mL). The

mixture was stirred at room temperature during 24 h. The reaction mixture was quenched with a saturated solution of NH_4Cl and CH_2Cl_2 was added. The aqueous layer was extracted 3 times with CH_2Cl_2. Combined organic layers were dried over Na_2SO_4 and filtered. Concentration under reduced pressure afforded the crude product. The crude product was purified by flash chromatography over silica gel (acetone/toluene 20/80 to 30/70) and precipitated in pentane to afford amide **5** as a white solid (682 mg, 1.14 mmol, 76% over 2 steps from 1).

Mp: 96–100 °C; Rf = 0.44 (A/T 30/70); IR (ATR) ν_{max} (cm^{-1}) 3324, 2923, 2854, 1695, 1646, 1547, 1466, 1404, 1370, 1328, 1276, 1200, 1162, 1138, 1082, 1059, 960, 900, 801, 737, 697, 650, 605, 559, 492, 426; ^{1}H-NMR (300 MHz, $CDCl_3$) δ (ppm) 9.75 (s, 1H, NH-3), 7.38–7.21 (m, 6H, H_6/$H_{aromatics}$), 6.26 (appearing t, J = 6.6 Hz, 1H, $H_{1'}$), 5.85 (t, J = 5.7 Hz, 1H, H_e), 4.50 (AB system, J = 11.7 Hz, 2H, $H_{a'}$), 4.40–4.30 (m, 1H, $H_{5'a}$), 4.27–4.18 (m, 2H, $H_{4'}$/$H_{5'b}$), 4.16–4.09 (m, 1H, $H_{3'}$), 3.17 (q, J = 6.6 Hz, 2H, H_f), 2.77–2.54 (m, 2H, H_c), 2.52–2.36 (m, 3H, $H_{2'a}$/H_b), 2.15–2.01 (m, 1H, $H_{2'b}$), 1.89 (appearing s, 3H, H_7), 1.52–1.37 (m, 2H, H_g), 1.33–1.11 (m, 18H, $H_{aliphatics}$), 0.92–0.76 (m, 3H, H_h); ^{13}C-NMR (75.5 MHz, $CDCl_3$) δ (ppm) 172.7 (C_a), 170.9 (C_d), 164.1 (C_4), 150.5 (C_2), 137.3 ($C_{b'}$), 135.4 (C_6), 128.6 ($C_{d'}$), 128.0 ($C_{e'}$), 127.7 ($C_{c'}$), 111.2 (C_5), 85.2 ($C_{1'}$), 82.2 ($C_{4'}$), 78.5 ($C_{3'}$), 71.7 ($C_{a'}$), 64.0 ($C_{5'}$), 39.7 (C_f), 37.5 ($C_{2'}$), 31.9 ($C_{aliphatic}$), 30.6 (C_b), 29.6 (C_g), 29.6 ($C_{aliphatic}$), 29.6 ($C_{aliphatic}$), 29.6 ($C_{aliphatic}$), 29.4 ($C_{aliphatic}$), 29.3 ($C_{aliphatic}$), 29.3 (C_c), 26.9 ($C_{aliphatic}$), 22.7 ($C_{aliphatic}$), 14.1 (C_h), 12.6 (C_7); HRMS (ESI): Calcd for $C_{33}H_{49}N_3O_7$ $[M + H]^+$, 600.36488, found 600.36449.

Preparation of the oleogels and characterization

Gel formation. Medium chain triglyceride oil (MCT), Miglyol® 812 N, was chosen as the oil vehicle as a generally recognized as safe (GRAS) excipient for lipidic pharmaceutical formulations. It was kindly provided by IOI Oleo GmbH (Hambourg, Germany).

Synthetic NL gelators were dispersed in oil to a minimum concentration and minimum temperature to achieve their complete dissolution. The critical gelation concentration (CGC) was quantitatively assessed by successively dissolving NLs in MCT oil (starting from 1% w/w) in a series of vials, heating and allowing them to rest at room temperature. In the case of oleogels, both thermomixer and ultrasonic bath techniques can be used to enhance gel formation and optimize self-assembly. Both technics were used for dissolution of each compound and the best one was finally selected. After preparation, the samples were tested by inversion of vials at ambient temperature. The lowest concentration at which there was no visually observable material flow was considered the critical concentration (in weight percent) and then defined as CGC.

NL **3** was unsuccessfully dissolved in the oil phase showing crystal suspension even at a concentration below 1% (w/w). The lack of dissolution did not allow further gelation and was not retained for further analysis. NL **4** was dissolved in MCT oil and the test-tube was heated at 70 °C for 2 cycles of 20 minutes (a total of 40 minutes) at 800 rpm until complete dissolution (Thermomixer compact, Eppendorf, Hauppauge, NY, USA) before being allowed to cool down to room temperature. Gel formation was observed at CGC of 16% (w/w) within 21 hours when the sample did not flow under its own weight using inversion tube method. The need to use a high concentration of gelator for oleogel formation resulted in NL **4** not being retained for further pharmaceutical development (see SI Fig. S1).

NL **5** was dissolved in Miglyol® 812 N and the test-tube was heated at 80 °C for 2 cycles of 10 minutes at 37.7 kHz until complete dissolution (Elmasonic P 30 H) before being allowed to cool down to room temperature. Gel formation was observed at CGC of 1.5% (w/w) within 1.5 hour when the sample did not flow under its own weight using the inversion tube method (see SI Fig. S2).

Gel characterization

Rheological study. Rheological measurements were performed on a Kinexus® Pro+ rheometer (Malvern Instruments Ltd., Orsay, France) with steel plate-plate geometry (diameter: 20 mm). The lower plate has a Peltier temperature control system and all gel samples were studied at ambient temperature (25 ± 0.01 °C) unless specified. The gel was placed on the bottom geometry using a plastic spatula and the oleogels rested for a 30 min equilibration before the experiments started. All measurements were carried out within the linear viscoelastic regime (LVR) involving no disruption of the gel structure. LVR was determined through an amplitude strain sweep experiment (shear strain: 0.001–100%, frequency: 12.57 rad.s^{-1} (2 Hz)). Elastic G′ and viscous G″ moduli were evaluated by performing a frequency sweep experiment from 0.1257 to 12.57 rad.s^{-1} at a shear strain of 0.1% (independence of moduli with the applied strain). At classical angular frequency of 1 Hz, the harmonic distortion values indicate a poor quality of the signal and therefore of the measurement (HD > 2%), which makes it unusable. Previous results of the literature reported higher angular frequency (10 rad.s^{-1}) for suitable characterization of organogels.[5] Thixotropic behavior was measured by a step-strain measurement composed of three steps repeated three times: 1) shear strain of 0.1% for 30 minutes (within the LVR), 2) shear strain of 10% for 2 minutes (outside of the LVR), 3) shear strain of 0.1% until stabilization (within the LVR).

The determination of gel–sol transition temperature Tgel/sol was determined by rheology. The oleogel (5% w/w NL **5**) was gradually heated from 25 to 85 °C at 0.1% shear strain (heating rate 5 °C min^{-1}). The gel–sol transition temperature was recorded at 79.5 °C as soon as the gel became liquid. At least three replicates were measured for each sample. (See SI).

Optical microscopy. Optical microscopy was performed using a Zeiss Axiovert 200 inverted light microscope linked to

an AxioCam MRm camera. Samples were observed between slide and slip cover without any staining.

Nanoemulsion preparation and characterization

NEs formulation. NE manufactured in this work were oil in water NE with 20% of oil phase. Oil phase manufacturing process consisted in the dispersion of egg lecithin (Lipoid® E80) and NL in MCT oil (Miglyol® 812 N). The aqueous phase was composed of distilled water and polysorbate 80 (Tween® 80). Both phases were heated separately prior emulsification to 70 °C in water bath.

Emulsification was accomplished by phase inversion and nanoemulsion (oil droplets in submicronic size range) was finally obtained by 8 minutes sonication using a Branson Ultrasonic Sonifier S-250A set at 35% and output 1.5. Prior to gelation, a sample of NE was retained for further granulometric analysis. Gelation of the NE was then observed within 2 hours.

NEs characterization. NE was visually inspected for eventual creaming, phase separation and/or precipitation. Granulometric characteristics of all NEs were assessed by dynamic light scattering (DLS) using Malvern instruments (Zetasizer Nano ZS) before gelation. NEs were diluted at 1 : 1500 (v/v) in distilled water, and the average size and the polydispersity index were determined by three independent measurements performed at 25 °C. To analyze the ζ-potential, NEs were diluted at 1 : 1500 (v/v) in distilled water, and measurements were performed using Zetasizer Nano ZS coupled with a folded capillary cell (DTS1060) from Malvern Instruments. Colloidal stability of non-gelled NEs has been demonstrated for at least three months. The droplet's mean diameter, index of polydispersity, and ζ-potential remained stable during the study. Optical microscopic observation of the gelled NE was performed as previously described for gel. The stability of the gelled NE was assessed by visual observation The main paragraph text follows directly on here.

Rheological study. Rheological characterization of gelled NE was performed as previously described for oleogel with a Kinexus® Pro+ rheometer (Malvern Instruments Ltd., Orsay, France) with steel plate-plate geometry (diameter: 20 mm) at an angular frequency of 2 Hz. Elastic G′ and viscous G″ moduli were evaluated by performing a frequency sweep experiment from 0.1257 to 12.57 rad.s^{-1} at a shear strain of 0.1% (independence of moduli with the applied strain) see SI Fig. S8A and S8B.

***In vitro* cytotoxicity assay.** A MTS tetrazolium assay was performed on immortalized keratinocyte cell line. Cells were plated at 2000 cells by well in 96 well plates in keratinocyte growth medium-2 (KGM™-2, Promocell). Due to the lipophilic chemical characteristic of the oleogelator, the NL **5** was prior contact with cells formulated in oil-in-water (o/w) NE at 2% and diluted in culture medium at 1/1000e (v/v). The cell cultures were kept at 37 °C, 5% CO_2 for 24 hours prior to NE exposure, to allow the cells to attach to the microplate. Prior to incubation, the cells were washed with 200 μL phosphate-buffered saline (PBS); then, 100 μL of dilution of emulsion was distributed in the wells, and plates were incubated for 4 hours, 24 and 48 hours at 37 °C, 5% CO_2. After incubation times, NE was removed and the cells were rinsed with 200 μL of PBS. MTS were performed 4 h, 24 h and 48 h after treatment. MTS is based on the conversion of a tetrazolium salt into a colored formazan product by mitochondrial activity of viable cells at 37 °C. The amount of formazan which is directly proportional to the number of living cells in culture was measured at 492 nm by microplate reader. Optical density (OD) results were compared with the control cells not exposed to NE-NL **5**. (SI Fig. S12).

Conclusions

In conclusion, this manuscript presents an innovative molecular approach utilizing a simple and efficient synthetic sequence for the development of a versatile supramolecular oleogelator derived from nucleolipids (NL) and its application in the formulation of gelled nanoemulsions. These results emphasize the significance of structural factors in the gelation processes and shed light on the molecular properties governing self-assembly and gelation. The NL **5** oleogelator, containing a 1,4-dicarbonyl ester-amide linkage, demonstrated unprecedented self-assembly properties, leading to the first NL-based low molecular weight oleogel (LMWO). Forming a three-dimensional solid-like network, NL **5** effectively stabilized triglyceride-based oleogels at remarkably low concentrations. Additionally, it induced the gelling of an oil-in-water nanoemulsion, resulting in a novel oleogel-based nanoemulsion through supramolecular interactions. The design of this low molecular weight oleogelator based on nucleolipids opens new avenues for soft materials in various applications, providing advantages over traditional organogels and hydrogels. Particularly, organogels have been sparingly used for parenteral drug delivery due to the scarcity of high-quality pharmaceutical carriers. The biocompatibility and biodegradability of such a simple NL-based oleogelator make it highly attractive for pharmaceutical and cosmetic developments. Indeed, the 1,4-dicarbonyl linkage is formed from ester and amide functions, both of which are known to be easily cleaved by esterases or amidases found *in vivo*. Regarding biocompatibility, the non-cytotoxicity of the synthetic NL has been confirmed and is illustrated by the MTS assay results, which are presented in the SI. Moreover, the final formulation was designed using only excipients that are generally recognised as safe (GRAS): Miglyol® 812 N, Lipoid E80® and Tween® 80. This design choice was critical for achieving efficient clinical translation. This study highlights the potential of oleogels as safe and effective biomaterials for controlled administration of hydrophobic pharmaceuticals. It paves the way for biodegradable systems intended for parenteral, oral, and topical administration to enhance drug bioavailability, stability, and sustained release.

Author contributions

Conceptualization: VD, SCM, CP. Data curation: AKE, BD, AS, NM, BK, MC, FC. Formal analysis: AKE, BD, AS, NM, AL, BK, MC, FC, VD, SCM. Funding acquisition: VD, SCM, CP. Investigation: AKE, BD, AS, NM, BK, MC, FC. Methodology: AKE, BD, AL, BK, VD, SCM. Project administration: VD, SCM, CP. Resources: VD, SCM, BK, PB, AL, MC. Supervision: VD, SCM. Validation: AL, BK, PB, FC, VD, SCM. Visualization: VD, AKE, BD, MC, BK. Writing – original draft: VD, SCM. Writing – review & editing: VD, SCM, AKE, BD, AL, BK, PB, FC, CP.

Conflicts of interest

There are no conflicts to declare.

Data availability

All data supporting the findings of this study are included within the article and its supplementary information (SI).

Supplementary information is available. See DOI: https://doi.org/10.1039/d5me00074b.

CCDC 2386437 and 2386438 (**3** and **4**) contain the supplementary crystallographic data for this paper.[77a,b]

Acknowledgements

A. K. E. thanks the Agence Innovation Defense (AID) for Ph. D grant and Dr. Colonel C. Piérard for mentorship. B. D. thanks the French MESRI for Ph. D grant. We thank the CNRS and the INSERM for financial support. E. A. Willemaers is acknowledged for her help in optical microscopy. HRMS, DRX and solid NMR studies were performed at IECB, Bordeaux. This work benefited from the facilities and expertise of the Biophysical and Structural Chemistry platform at IECB, CNRS UMS3033, INSERMUS001, and Bordeaux University, France.

Notes and references

1 S. Zhang, *Nat. Biotechnol.*, 2003, **21**, 1171.
2 J. W. Steed, *Chem. Commun.*, 2011, **47**, 1379.
3 L. E. Buerkle and S. J. Rowan, *Chem. Soc. Rev.*, 2012, **41**, 6089.
4 R. G. Weiss, *J. Am. Chem. Soc.*, 2014, **136**, 7519.
5 J. Raeburn and D. J. Adams, *Chem. Commun.*, 2015, **51**, 5170.
6 D. L. Taylor and M. In Het Panhuis, *Adv. Mater.*, 2016, **28**, 9060.
7 E. R. Draper and D. J. Adams, *Chem*, 2017, **3**, 390.
8 M. Liu, G. Ouyang, D. Niu and Y. Sang, *Org. Chem. Front.*, 2018, **5**, 2885.
9 D. J. Adams, *J. Am. Chem. Soc.*, 2022, **144**, 11047.
10 X. Du, J. Zhou and B. Xu, *Chem. – Asian J.*, 2014, **9**, 1446.
11 M. Zhang and R. G. Weiss, *J. Braz. Chem. Soc.*, 2016, **27**, 239.
12 F. Khan and S. Das, *ChemistrySelect*, 2022, **7**, e202200205.
13 H. Wang, Z. Yang and D. J. Adams, *Mater. Today*, 2012, **15**, 500.
14 C. Kraaz and N. Castellucci, *Chem. Soc. Rev.*, 2013, **42**, 156.
15 S. C. Lange, J. Unsleber, P. Drucker, H. J. Galla, M. P. Waller and B. J. Ravoo, *Org. Biomol. Chem.*, 2015, **13**, 561.
16 N. Falcone and H.-B. Kraatz, *Chem. – Eur. J.*, 2018, **24**, 1.
17 E. R. Draper and D. J. Adams, *Langmuir*, 2019, **35**, 6506–6521.
18 T. Shao, N. Falcone and H.-B. Kraatz, *ACS Omega*, 2020, **5**, 1312.
19 J. F. Arokianathan, K. A. Ramya, A. P. Deshpande, A. Leemarose and G. Shanmugam, *Colloids Surf., A*, 2021, **618**, 1–9.
20 B. Pramanik and S. Ahmed, *Gels*, 2022, **8**, 533.
21 N. Basu, A. Chakraborty and R. Ghosh, *Gels*, 2018, **4**, 52.
22 A. Prathap and K. M. Sureshan, *Langmuir*, 2019, **35**, 6005.
23 A. Chalard, P. Joseph, S. Souleille, B. Lonetti, N. Saffon-Merceron, I. Loubinoux, L. Vaysse, L. Malaquin and J. Fitremann, *Nanoscale*, 2019, **11**, 15043.
24 F. Ono, K. Ichimaru, O. Hirata, S. Shinkai and H. Watanabe, *Chem. Lett.*, 2020, **49**, 156.
25 J. Morris, J. Bietsch, K. Bashaw and G. Wang, *Gels*, 2021, **7**, 24.
26 P. Barthélémy, *C. R. Chim.*, 2009, **12**, 171.
27 M. Peters and J. T. Davis, *Chem. Soc. Rev.*, 2016, **45**, 3188.
28 Y. Zhang, L. Zhu, J. Tian, L. Zhu, X. Ma, X. He, K. Huang, F. Ren and W. Xu, *Adv. Sci.*, 2021, **8**, 2100216.
29 B. Alies, M. A. Ouelhazi, A. Patwa, J. Verget, L. Navailles, V. Desvergnes and P. Barthélémy, *Org. Biomol. Chem.*, 2018, **16**, 4888.
30 M. Sicard, S. Crauste-Manciet, F. Dole, J. Verget, A. Thiéry and P. Barthélémy, *ACS Sustainable Chem. Eng.*, 2020, **8**, 11052.
31 A. Nuthanakanti and S. G. Srivatsan, *Nanoscale Adv.*, 2020, **2**, 4161.
32 A. Nuthanakanti and S. G. Srivatsan, *Nanoscale*, 2016, **8**, 3607.
33 D. Jain, A. Karajic, M. Murawska, B. Goudeau, S. Bichon, S. Gounel, N. Mano, A. Kuhn and P. Barthélémy, *ACS Appl. Mater. Interfaces*, 2017, **9**, 1093.
34 T. Coradin, M. Boissière and J. Livage, *Curr. Med. Chem.*, 2006, **13**, 99.
35 H. Rosemeyer, *Chem. Biodiversity*, 2005, **2**, 977.
36 A. Gissot, M. Camplo, M. W. Grinstaff and P. Barthelemy, *Org. Biomol. Chem.*, 2008, **6**, 1324.
37 J. Baillet, V. Desvergnes, A. Hamoud, L. Latxague and P. Barthélémy, *Adv. Mater.*, 2018, **30**, 1705078.
38 L. Moreau, M. Camplo, M. Wathier, N. Taib, M. Laguerre, I. Bestel, M. W. Grinstaff and P. Barthélémy, *J. Am. Chem. Soc.*, 2008, **130**, 14454.
39 A. Allain, C. Bourgaux and P. Couvreur, *Nucleic Acids Res.*, 2012, **40**, 1891.
40 C. Montis, Y. Gerelli, G. Fragneto, T. Nylander, P. Baglioni and D. Berti, *Colloids Surf., B*, 2016, **137**, 203.
41 A. Nuthanakanti, M. B. Walunj, A. Torris, M. V. Badigerb and S. G. Srivatsan, *Nanoscale*, 2019, **11**, 11956.
42 M. B. Walunj, S. Dutta and S. G. Srivatsan, in *Molecular Architectonics and Nanoarchitectonics. Nanostructure Science and Technology*, ed. T. Govindaraju and K. Ariga, Springer, Singapore, 2022.

43 N. M. Sangeetha and U. Maitra, *Chem. Soc. Rev.*, 2005, **34**, 821.
44 M. G. F. Angelerou, P. W. J. M. Frederix, M. Wallace, B. Yang, A. Rodger, D. J. Adams, M. Marlow and M. Zelzer, *Langmuir*, 2018, **23**, 6912.
45 P. R. A. Chivers and D. K. Smith, *Nat. Rev. Mater.*, 2019, **4**, 463.
46 M. B. Walunj and S. G. Srivatsan, *Chem. – Asian J.*, 2022, **17**, e202101163.
47 C. L. Esposito, P. Kirilov and V. G. Roullin, *J. Controlled Release*, 2018, **271**, 1.
48 M. Davidovich-Pinhas, *Ther. Delivery*, 2015, **7**, 1.
49 P. Terech and R. G. Weiss, *Chem. Rev.*, 1997, **97**, 3133.
50 L. S. K. Dassanayake, D. R. Kodali and S. Ueno, *Curr. Opin. Colloid Interface Sci.*, 2011, **16**, 432.
51 J. Yan, B. S. Wong and L. Kang, in *Soft Fibrillar Materials: Fabrication and Applications*, ed. X. Y. Liu and J.-L. Li, Wiley-VCH Verlag GmbH & Co. KGaA, 1st edn, 2012.
52 R. Balasubramanian, A. A. Sughir and G. Damodar, *Asian J. Pharm.*, 2012, **6**, 1.
53 L. Li, G. Liu, O. Bogojevic, J. N. Perdersen and Z. Guo, *Compr. Rev. Food Sci. Food Saf.*, 2022, **21**, 2077.
54 L. Moreau, P. Barthélémy, M. El Maataoui and M. W. Grinstaff, *J. Am. Chem. Soc.*, 2004, **126**, 7533.
55 G. Godeau and P. Barthélémy, *Langmuir*, 2009, **25**, 8447.
56 B. Dessane, R. Smirani, G. Bouguéon, T. Kauss, E. Ribot, R. Devillard, P. Barthélémy, A. Naveau and S. Crauste-Manciet, *Sci. Rep.*, 2020, **10**, 2850.
57 R. J. Wilson, Y. Li, Y. Guangze and C.-X. Zhao, *Particuology*, 2021, **64**, 85.
58 D. J. McClements, *Soft Matter*, 2012, **8**, 1719.
59 M. Z. Ahmad, J. Ahmad, M. Y. Alasmary, S. Akhter, M. Aslam, K. Pathak, P. Jamil and M. M. Abdullah, *J. Drug Delivery Sci. Technol.*, 2022, **72**, 103420.
60 M. R. Donthi, S. R. Munnangi, K. V. Krishna, R. N. Saha, G. Singhvi and S. K. Dubey, *Pharmaceutics*, 2023, **15**, 164.
61 M. Miastkowska, A. Kulawik-Pióro, E. Lasoń, K. Śliwa, M. A. Malinowska, E. Sikora, T. Kantyka, E. Bielecka, A. Maksylewicz, E. Klimaszewska, M. Ogorzałek, M. Tabaszewska, L. Skoczylas and K. Nowak, *Pharmaceutics*, 2023, **15**, 2559.
62 F. Delbecq, R. Nguyen, E. Van Hecke and C. Len, *J. Mol. Liq.*, 2019, **295**, 111708.
63 D. M. Zurcher and A. J. McNeil, *J. Org. Chem.*, 2015, **80**, 2473.
64 M. A. Catry and A. Madder, *Molecules*, 2007, **12**, 114.
65 W. J. Peveler, H. Packman, S. Alexander, R. R. Chauhan, L. M. Hayes, T. J. Macdonald, J. K. Cockcroft, S. Rogers, D. G. A. L. Aarts, C. J. Carmalt, I. P. Parkin and J. C. Bear, *Soft Matter*, 2018, **14**, 8821.
66 V. A. Mallia and R. G. Weiss, *J. Phys. Org. Chem.*, 2014, **27**, 310.
67 F. Delbecq, K. Tsujimoto, Y. Ogue, H. Endo and T. Kawai, *J. Colloid Interface Sci.*, 2013, **390**, 17.
68 T. Shimizu, R. Iwaura, M. Masuda, T. Hanada and K. Yase, *J. Am. Chem. Soc.*, 2001, **123**, 5947.
69 G. Godeau, J. Bernard, C. Staedel and P. Barthélémy, *Chem. Commun.*, 2009, 5127.
70 Y. J. Yun, S. M. Park and B. H. Kim, *Chem. Commun.*, 2003, 254.
71 L. Meng, K. Liu, S. Mo, Y. Mao and T. Yi, *Org. Biomol. Chem.*, 2013, **11**, 1525.
72 T. C. Pinto, A. J. Martins, L. Pastrana, M. C. Pereira and M. A. Cerqueira, *Gels*, 2021, **7**, 86.
73 A. Martín-Illana, F. Notario-Pérez, R. Cazorla-Luna, R. Ruiz-Caro, M. C. Bonferoni, A. Tamayo and M. D. Veiga, *Drug Discovery Today*, 2022, **27**, 1008.
74 V. Nouri, M. Pontes De Siqueira Moura, B. Payre, O. De Almeida, C. Déjugnat, S. Franceschi and E. Perez, *Soft Matter*, 2020, **16**, 2371.
75 A.-L. Fameau, F. Cousin, I. Dobryden, C. Dutot, C. Le Coeur, J.-P. Doiliez, S. Prevost, B. P. Binks and A. Saint-Jalmes, *J. Colloid Interface Sci.*, 2024, **672**, 133.
76 P. K. Okuro, A. A. Malfatti-Gasperini, A. A. Vicente and R. L. Cunha, *Food Res. Int.*, 2018, **111**, 168.
77 (*a*) CCDC 2386437: Experimental Crystal Structure Determination, 2025, DOI: 10.5517/ccdc.csd.cc2l38vv; (*b*) CCDC 2386438: Experimental Crystal Structure Determination, 2025, DOI: 10.5517/ccdc.csd.cc2l38ww.